

Scanning Tunneling Spectroscopy of C₃₆

Philip G. Collins, Jeffrey C. Grossman, Michel Côté, M. Ishigami, C. Piskoti, Steven G. Louie, Marvin L. Cohen, and A. Zettl

Department of Physics, University of California at Berkeley, and Materials Sciences Division, Lawrence Berkeley National Laboratory, Berkeley, California 94720

(Received 10 July 1998)

The local density of electronic states $N(E)$ has been measured on C₃₆ thin films using scanning tunneling spectroscopy (STS). A 0.8 eV energy gap and sharp features in $N(E)$ with widths as small as 0.2 eV can be ascribed to the discrete molecular energy levels predicted for the C₃₆ molecule, broadened by intermolecular interactions. However, a more complete agreement between the experimental results and theoretical predictions occurs if the system is modeled as covalently bonded C₃₆ dimers and trimers. These results confirm the molecular nature of C₃₆ as well as its higher reactivity as compared to larger size fullerenes. [S0031-9007(98)08156-3]

PACS numbers: 73.61.Wp, 61.16.Ch, 71.20.Tx

The discovery of fullerenes [1], along with their synthesis in bulk [2], has generated a multidisciplinary research effort. The recent identification and isolation of the C₃₆ molecule [3] now allows us to study a caged fullerene smaller than C₆₀, increasing our understanding of these novel forms of carbon.

In particular, questions regarding superconductivity are of interest for this new, smaller molecule. Alkali-intercalated C₆₀ has an anomalously high superconducting transition temperature T_c [4]. Two properties which contribute to this high T_c are the strong electron-phonon coupling and a sharply peaked density of electronic states $N(E)$ due to the molecular nature of solid C₆₀ [5]. By curvature arguments alone [6,7], the smaller, more strained C₃₆ molecule should have a higher electron-phonon coupling. Recent first-principles calculations confirm that a C₃₆ solid may have an enhanced T_c over the A₃C₆₀ compounds [8].

We have performed scanning tunneling spectroscopy (STS) studies of C₃₆ islands to elucidate the electronic structure of C₃₆. In particular, we have sought to determine whether C₃₆ forms a molecular or a covalent solid, and to determine the relative magnitudes of features in $N(E)$ which might contribute to superconductivity in a solid crystal. The experimental results have prompted consideration of various bonding arrangements between C₃₆ molecules, some of which have theoretical $N(E)$ which closely match the experimental results.

The C₃₆ powder was synthesized using a plasma-arc technique and subsequently purified as described by Piskoti *et al.* [3]. The powder was then outgassed and thermally evaporated onto atomically flat Au(111) films deposited on mica substrates. Short, intense heating was used to evaporate our films because, in slowly evaporated films, the C₃₆ molecules thermally disintegrate before subliming, matching the behavior of similarly strained endohedral fullerenes [9]. Our method tends to eject intact C₃₆ molecules towards the substrate as confirmed

by electron diffraction studies of the films [3]. Using a mechanical shutter, very low coverages between 0.1 and 1 monolayer of C₃₆ could be obtained.

The films were immediately loaded into a scanning tunneling microscope, operating at room temperature with a Pt-Ir tunneling tip. The position of the tunneling tip could be fixed directly over any feature on the surface. With the feedback loop disabled, current-voltage (I - V) curves were repeatedly acquired, averaged, and then numerically differentiated. The resulting dI/dV curves, which are proportional to $N(E)$ for single electron tunneling, identified position-dependent electronic features. As is conventional on semiconductor surfaces [10], the logarithmic derivative $(V/I) dI/dV$ was employed for features which displayed vanishingly small currents.

To provide confirmation of our results, solvated C₃₆ was also applied to clean Au(111) films and highly oriented pyrolytic graphite (HOPG) crystals. Using both tunneling microscopy and spectroscopy, the pure solvent was found to evaporate cleanly, having no electronic effect on the surfaces. C₃₆ films produced by the two methods were indistinguishable on the Au substrates, and the only observable difference on HOPG appears to be characteristic of that surface, as will be described below.

Whether prepared from solution or by thermal evaporation, the C₃₆ molecules tend to aggregate into islands. Typical island diameters in this study ranged from 10 to 50 nm. The true height of the islands is more difficult to determine from topographic data, which actually represent the movement of the tunneling tip as it tries to maintain a constant tunneling current. At low sample biases the islands are nearly electronically transparent, so the apparent island height approaches zero. At sample biases of 1.0 to 1.5 V, on the other hand, the islands contribute strongly to the tunneling current and the tip response can be tens of Angstroms. Similarly, there is a bias dependence to the observation of tip contamination. At low bias, the tip is easily contaminated and surface features are often modified

by scanning. At higher biases, surface features are unchanged and the electronic nature of the tip is more stable, as determined by spectroscopy on a bare gold region of the surface.

At some point between these two regimes, the tip follows the C_{36} island topography most accurately. At the threshold of tip contamination, the tip is nearly in contact with the islands. By measuring this height, we estimate the typical C_{36} island to be between 10 and 20 Å high, independent of diameter. Since the C_{36} molecule itself is 5 to 6 Å tall, depending on how it sits on the substrate, these islands are apparently 2 to 4 molecules high. This clustering indicates an attractive interaction between the C_{36} molecules and a relatively weaker interaction between the adsorbed molecules and the substrate. Despite this tendency to coalesce, the C_{36} islands are rarely well ordered or smooth. Crystalline ordering of the island may be frustrated both by a random orientation of the molecules on the substrate and by the low temperature of the substrate during sample preparation. Preliminary attempts to anneal similar films led to a complete loss of observed electron diffraction peaks, indicating a breakdown of the fullerene cage structure.

Figure 1 depicts the tunneling differential conductivity dI/dV observed over a C_{36} island and on the bare Au substrate. The data are an average of multiple spectra taken at various positions either on or off of the island. The density of states for a good metal like Au is flat, resulting in a featureless dI/dV curve [11]. At energies near the Fermi level, the C_{36} -covered Au appears identical to the bare Au, indicating the extent to which C_{36} is electronically transparent. At higher biases the C_{36} island causes sharp increases, as much as fivefold, in the tunneling current. These increases produce well-resolved peaks in the measured dI/dV curves. The width of these peaks is of the order of 200 mV, suggesting that they arise from reso-

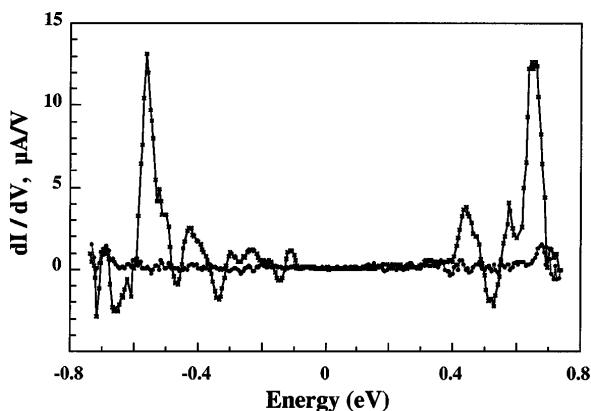


FIG. 1. Differential conductivity of a bare Au surface and a C_{36} -covered Au surface. The difference between the two curves clearly delineates electronic features of the C_{36} molecules, including an 0.8 eV electronic gap. The data were acquired after stabilizing the tip with a 0.75 V sample bias and 0.5 nA tunneling current.

nant tunneling to discrete electronic states between the tip and the Au surface. Since these states appear only over C_{36} islands, the discrete states correspond to the C_{36} molecules which, despite clustering tendencies, retain molecularlike electronic states.

Figure 2 displays results obtained on Au over a wider 3 V energy range, and compares these results to those obtained on HOPG. On both substrates, the additional $N(E)$ attributed to C_{36} molecules appears as a collection of sharp electronic features. By identifying similarities between the two curves, a number of discrete states above and below the Fermi level may be identified. On both substrates, three narrow, occupied states are measured at -1200 , -550 , and -450 meV; an electronic gap, in which C_{36} contributes no current, is observed between -400 and 400 meV; and above the Fermi level empty electronic states lie at 450 , 800 , and 1300 meV. Additional features, such as the peak at -900 meV, are stronger on one substrate than another and are more difficult to reliably define. With dark lines at the top of the figure, we mark peaks and apparent peak widths which are most reproducibly observed on both substrates.

The only significant difference between the results on the two substrates is the relative weakness of C_{36} features on HOPG between 500 and 1000 meV. On close inspection, both $N(E)$ curves are peaked at the same energies, but are only 10 to 20% as high on HOPG as for the Au substrate. Since the features are unshifted, the apparent loss of states observed on HOPG may be simply due to orientation. For instance, the C_{36} molecules could prefer to stand upright on the Au substrate but lay flat on the

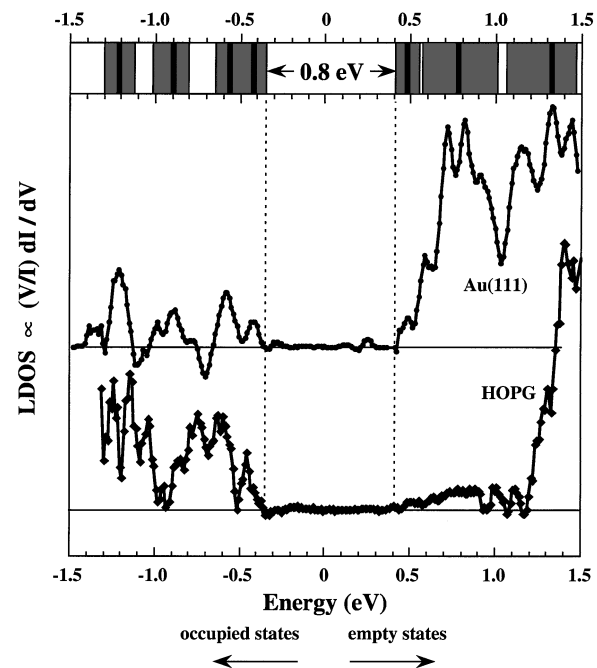


FIG. 2. $N(E)$ for C_{36} as measured on Au(111) and HOPG substrates. Discrete states above and below the electronic gap have similar energies for both substrates.

HOPG. Other, more complex interactions such as differences in substrate bonding or charge transfer may also be contributing. In particular, registry between the hexagonal substrate and the C_{36} hexagon ring could amplify the effects of interfering current paths for a C_{36} -derived, unoccupied molecular orbital. If further vacuum tunneling studies reproduce this substrate-induced effect, then a more refined theoretical treatment can be pursued.

Theoretical local-density approximation (LDA) calculations [12] for isolated D_{6h} symmetry C_{36} molecules compare favorably with these results and are reproduced at the top of Fig. 4. After accounting for the standard LDA underestimation of the energy gap, the experimental and theoretical spectra match closely near the Fermi level. The theoretical energy spacing between the two lowest unoccupied and two highest occupied molecular levels, as well as the relative spectral weights of these levels, are all reproduced by the experimental data.

However, there is serious disagreement between experiment and theory further from the Fermi level: in LDA, the isolated molecule has no eigenvalues in the +1.0 to +2.0 eV and the -1.0 to -2.0 eV energy ranges, while a number of states appear to be present experimentally. There are a number of effects which may explain such a discrepancy, including (i) bonding between C_{36} units, (ii) impurities in the sample, and (iii) passivation of the C_{36} molecules by other species. Previous calculations [8] have predicted C_{36} molecules to be more reactive than larger fullerenes like C_{60} , even to the extent that stable covalently bonded crystals may be formed. Although impurities and passivation cannot be absolutely ruled out, the vacuum environment in which the samples were produced would favor intermolecular bonding as the most likely cause of deviation from isolated molecule behavior, particularly considering that the molecules are mobile enough to cluster into islands.

To investigate the possible effects of intermolecular bonding, a series of calculations have been carried out for a variety of C_{36} dimers and trimers. Electronic and structural properties are calculated with DMOL version 960 [13] using the frozen-core approximation, a fine integration grid mesh, and double numerical-plus-polarization basis sets. All geometries are fully relaxed within the given symmetries. Dimerization was tested at each of the three inequivalent sites of the C_{36} molecule, with either one or two single bonds between two C_{36} molecules. Stable dimer formation occurred between C atoms located on the top hexagon or on the pentagon ring, but not for the third inequivalent site on the middle hexagon belt. In fact, completely unbonded dimers resulted from the latter case.

Figure 3 depicts three of the different dimers $(C_{36})_2$ -A, $(C_{36})_2$ -B, and $(C_{36})_2$ -C (hereafter referred to as dimers A, B, and C) and one of the trimers $(C_{36})_3$ considered in this work. Below each unit is the relevant symmetry and calculated binding energy. In all cases, the intermolecular bond distances can be considered as single C-C covalent

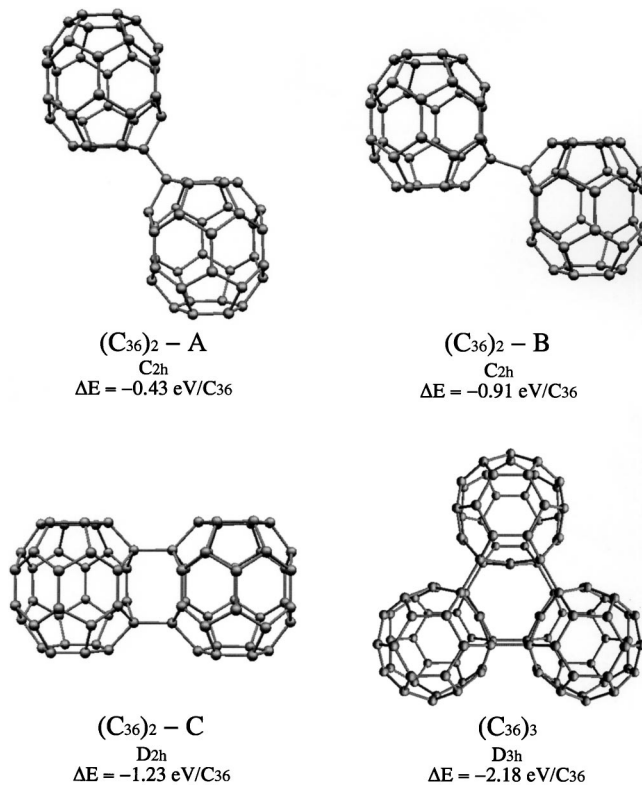


FIG. 3. Three different configurations of C_{36} dimers, and a C_{36} trimer, with their corresponding symmetries and binding energies with respect to isolated C_{36} molecules. To clarify the structure of the trimer, the z axis has been rotated.

bonds with an average length of 1.56 Å. Bonding which involves sites on the pentagon ring appear more favorable than bonding involving atoms on the top hexagon sites, but all of the configurations shown are energetically bound with respect to isolated molecules. Note that dimer C, which is the most stable configuration, can be obtained from dimer B simply by rotating one of the C_{36} units without breaking an existing bond.

The molecular orbital energy spectra in Fig. 4 indicate how sensitive the eigenvalue spectrum is to the nature of the intermolecular bonding. To facilitate comparison with the experimental results, a small, unweighted Lorentzian broadening is employed and each spectrum has been shifted so that the middle of the highest occupied–lowest occupied molecular orbital (HOMO-LUMO) gap lies at 0 eV. Doubly degenerate levels are counted twice so that relative peak heights are meaningful. In dimers A and B, a small gap (0.01 eV) results in a metallic eigenvalue spectrum. Dimer C, on the other hand, has a gap that is roughly the same as in the isolated molecule, shown at the top of the figure.

The experimental data in Fig. 2 may now be directly compared to the various theoretical spectra of Fig. 4. Neither dimers A nor B have the appropriate gap, as found for the isolated C_{36} molecule or dimer C. Although the isolated molecule fits the experimental data reasonably,

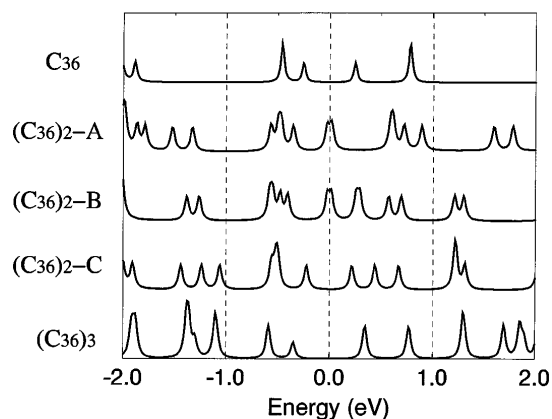


FIG. 4. Theoretical electronic spectra for five different configurations of C_{36} molecules, including an isolated molecule, three different C_{36} dimers, and a C_{36} trimer. As described in the text, a similar bonding configuration leads the bottom two spectra to be similar. Qualitatively, these spectra provide the best match to the experimental data.

as described above, dimer *C* possesses a more even distribution of states in the range of 1 to 2 eV above and below the Fermi level. This particular dimer, therefore, resolves the primary discrepancy between the experimental data and the isolated-molecule energy spectrum. Since it is also considerably well bound energetically, it strongly suggests that the C_{36} molecules are dimerized rather than isolated in this study.

Because the theoretical energy spectrum was found to be so sensitive to the bonding configuration, a number of other models were also considered. Spectra calculated for two different hydrogen-passivated $C_{36}H_6$ molecules matched the experimental data poorly. Three different trimer configurations were also considered, two of which were easily ruled out. A third trimer configuration, depicted as $(C_{36})_3$ in Figs. 3 and 4, bonds in a similar manner as dimer *C*, forming a threefold symmetric plane of C_{36} molecules. This particular trimer has an electronic spectrum similar to that of dimer *C* except for an increase of the gap at the Fermi level. Dimer *C* can be considered as the basic structural unit from which the important electronic features are derived.

We therefore conclude that this particular bonding configuration, either in the form of dimers or trimers, may be a dominant characteristic of the C_{36} islands in this study. Dimer *C* and the trimer are the most energetically favorable of the different molecular orientations calculated, including that of unbonded molecules. Qualitatively, both structures fit the electronic features of the experimental data, significantly more so than the isolated molecule spectrum or any of the other bonded molecules we have considered. And, finally, the formation of C_{36} dimers and trimers naturally explains the topographical disorder observed for the C_{36} islands, since short-range corrugations and lack of long-range order would immediately result

from random dimerization, coupled with frustration by the surface. Spontaneous dimerization is favored by the large 1–2 eV binding energies predicted. However, other mechanisms may also play a role in dimerization, as they do with C_{60} molecules [14,15].

In conclusion, we have measured sharp HOMO and LUMO features in the density of states for C_{36} islands and an 0.8 eV electronic gap. These features appear to correspond to discrete energy levels of C_{36} molecules. Additional states observed outside the gap do not occur in the isolated molecule spectrum but may be attributed to a particular dimerization configuration with D_{2h} symmetry proposed here.

While these results are suggestive, it should be stressed that dimerization is only one explanation for the differences between experimental and the isolated molecule spectra. As mentioned above, other possible effects can also change the energy spectrum dramatically. *In situ* preparation and analysis are still needed to conclusively rule out these other mechanisms, and atomic-resolution studies are necessary to identify the electronic effects of molecular orientation on a particular surface. Nonetheless, the results of our calculations on C_{36} dimers improve the present understanding of how solid state C_{36} may form and stabilize. Furthermore, the clearly observed band gap reveals that C_{36} , like C_{60} , will require additional doping in order to reach a metallic state.

This work was supported in part by a U.C. Berkeley Chancellor's Initiative Grant, NSF Grants No. DMR-9501156, No. DMR-9404755, and No. DMR-9520554, and by the Director of the Office of Energy Research, Office of Basic Energy Sciences, Materials Sciences Division of the U.S. DOE, Contract No. DE-AC03-76SF00098. Computational resources have been provided by NCSA. P.G.C. acknowledges support from a Helmholtz Fellowship and M.I. acknowledges support from the Hertz Foundation.

- [1] H. W. Kroto *et al.*, Nature (London) **318**, 162 (1985).
- [2] W. Kratschmer *et al.*, Nature (London) **347**, 354 (1990).
- [3] C. Piskoti, J. Yarger, and A. Zettl, Nature (London) **393**, 771 (1998).
- [4] A. F. Hebard *et al.*, Nature (London) **350**, 600 (1991).
- [5] O. Gunnarsson, Rev. Mod. Phys. **69**, 575 (1997).
- [6] M. Schluter *et al.*, Phys. Rev. Lett. **68**, 526 (1992).
- [7] J. L. Martins, Europhys. News **23**, 31 (1992).
- [8] M. Côté *et al.*, Phys. Rev. Lett. **81**, 697 (1998).
- [9] D. S. Bethune *et al.*, Nature (London) **366**, 123 (1993).
- [10] J. A. Stroscio and W. G. Kaiser, *Scanning Tunneling Microscopy* (Academic Press, New York, 1993), Vol. 27, pp. 460.
- [11] No Au surface states are resolved, in part due to the presence of C_{36} .
- [12] J. C. Grossman *et al.*, Chem. Phys. Lett. **284**, 644 (1998).
- [13] B. J. Delley, Chem. Phys. **92**, 508 (1990).
- [14] A. M. Rao *et al.*, Science **259**, 955 (1993).
- [15] S. Pekker *et al.*, Science **265**, 1077 (1994).